Atmos. Chem. Phys., 21, 7343–7355, 2021
https://doi.org/10.5194/acp-21-7343-2021

Atmospheric Chemistry and Physics
Open Access
EGU

Modeled changes in source contributions of particulate matter during the COVID-19 pandemic in the Yangtze River Delta, China

Jinlong Ma[1], Juanyong Shen[2], Peng Wang[3], Shengqiang Zhu[1], Yu Wang[1], Pengfei Wang[4], Gehui Wang[5,6], Jianmin Chen[1,6], and Hongliang Zhang[1,6]

[1]Fudan Tyndall Center, Department of Environmental Science and Engineering, Fudan University, Shanghai 200438, China
[2]School of Environmental Science and Engineering, Shanghai Jiao Tong University, Shanghai 200240, China
[3]Department of Civil and Environmental Engineering, Hong Kong Polytechnic University, Hong Kong 99907, China
[4]Department of Civil and Environmental Engineering, Louisiana State University, Baton Rouge, LA 70803, USA
[5]Key Laboratory of Geographic Information Science, Ministry of Education, School of Geographic Sciences, East China Normal University, Shanghai 200241, China
[6]Institute of Eco-Chongming (IEC), East China Normal University, Shanghai 200062, China

Correspondence: Hongliang Zhang (zhanghl@fudan.edu.cn) and Jianmin Chen (jmchen@fudan.edu.cn)

Received: 11 September 2020 – Discussion started: 5 January 2021
Revised: 1 April 2021 – Accepted: 3 April 2021 – Published: 12 May 2021

Abstract. Within a short time after the outbreak of coronavirus disease 2019 (COVID-19) in Wuhan, Hubei, the Chinese government introduced a nationwide lockdown to prevent the spread of the pandemic. The quarantine measures have significantly decreased the anthropogenic activities, thus improving air quality. To study the impacts caused by the lockdown on specific source sectors and regions in the Yangtze River Delta (YRD), the Community Multiscale Air Quality (CMAQ) model was used to investigate the changes in source contributions to fine particulate matter ($PM_{2.5}$) from 23 January to 28 February 2020, based on different emission control cases. Compared to case 1 (without emission reductions), the total $PM_{2.5}$ mass for case 2 (with emission reductions) decreased by more than 20 % over the entire YRD, and the reduction ratios of its components were 15 %, 16 %, 20 %, 43 %, 34 %, and 35 % in primary organic aerosol (POA), elemental carbon (EC), sulfate, nitrate, ammonium, and secondary organic aerosol (SOA), respectively. The source apportionment results showed that $PM_{2.5}$ concentrations from transportation decreased by 40 %, while $PM_{2.5}$ concentrations from the residential and power sectors decreased by less than 10 % due to the lockdown. Although all sources decreased, the relative contribution changed differently. Contributions from the residential sector increased by more than 10 % to 35 %, while those in the industrial sector decreased by 33 %. Considering regional transport, the total $PM_{2.5}$ mass of all regions decreased 20 %–30 % in the YRD, with the largest decreased value of 5.0 $\mu g\,m^{-3}$ in Henan, Hebei, Beijing, and Tianjin (Ha-BTH). In Shanghai, the lower contributions from local emissions and regional transmission (mainly Shandong and Ha-BTH) led to the reduced $PM_{2.5}$. This study suggests adjustments of control measures for various sources and regions.

1 Introduction

Fine particulate matter ($PM_{2.5}$, an aerodynamic diameter of fewer than 2.5 µm) has been a great concern in China since 2013 due to its high levels and related health risks (Lelieveld et al., 2015; Huang et al., 2014; He and Christakos, 2018; Shang et al., 2018; Song et al., 2017, 2016; Yan et al., 2018; Du and Li, 2016; Liu et al., 2016; Shen et al., 2020a). To improve air quality, China has promulgated stringent emission control plans such as the Air Pollution Prevention and Control Action Plan, and $PM_{2.5}$ concentrations have been reduced significantly in different regions (Zheng et al., 2018; Cai et al., 2017; Zhang et al., 2016; Zheng et al., 2017). In the Yangtze River Delta (YRD), one of the largest economic centers, $PM_{2.5}$ concentrations were reduced by 34.3 % from 2013 to 2017 due to significant efforts (China, 2018). However, $PM_{2.5}$ concentrations are still much higher than the rec-

ommended annual mean criteria of $10\,\mu g\,m^{-3}$ by the World Health Organization (WHO). The significant reductions in emissions led to changes in the local and regional transport contributions of key pollutants. Consequently, the air quality strategies need further improvement according to the source apportionment results.

$PM_{2.5}$ is a complex mixture of primary particulate matter (PPM) components and secondary formed components, and its source apportionment is based on quantifying the contributions of different sources to all the components. Statistical methods based on observed $PM_{2.5}$ composition information, using source profiles of different emission sources and assuming that composition remains unchanged in the atmosphere, can only resolve contributions of different source sectors to PPM, leaving secondary components as a whole (Tao et al., 2014; Gao et al., 2016; Yao et al., 2016; Zhang et al., 2013; Zhu et al., 2018). Source-oriented chemical transport models (CTMs) are capable of investigating the contributions of both source sectors and regional transports to both PPM and secondary components (Wang et al., 2014; Ying et al., 2014; Wang et al., 2014; Yang et al., 2020). For instance, Hu et al. (2015) reported that local emissions accounted for the highest fraction of PPM compared to the regional transport in Shanghai. Zhang et al. (2012) showed that the power sector ($\sim 30\,\%$) was the predominant contributor to sulfate, a component of secondary inorganic aerosol (SIA), and the remaining contributions were from industrial and residential sectors in Shanghai. Liu et al. (2020) reported that the industry sector was the major secondary organic aerosol (SOA) emissions source, and, additionally, both regional transport and local emissions were critical to Shanghai. With source contributions changed, the information provided by these studies is not suitable for further reductions in $PM_{2.5}$ in the YRD. Therefore, updated source apportionment information is needed to support the formulation of further reduction policy.

To prevent the spread of the COVID-19 pandemic, the unprecedented nationwide lockdown has been implemented to limit anthropogenic activities since January 2020. As a result, anthropogenic emissions decreased drastically, especially in the transportation and industry sectors (P. Wang et al., 2020). As a natural experiment with high research values, this provides a valuable opportunity to understand pollution changes with extremely strict measures. Studies have reported significant decreases in $PM_{2.5}$ in the YRD based on absolute concentrations (Chen et al., 2020; Li et al., 2020; Chauhan and Singh, 2020; Yuan et al., 2020). However, it is not clear how the contributions of local sources and regional transport changed, and the conclusions reported in the mentioned literature cannot be used to design control strategies. Thus, it is critical to investigate changes in source sectors and regions during the COVID-19 pandemic.

In this study, a source-oriented version of the Community Multiscale Air Quality (CMAQ) model is used to determine the contributions of source sectors and regional transport to $PM_{2.5}$ in the YRD from 23 January to 28 February. The impacts of quarantine measures are estimated by comparing the contributions before and after 23 January, the starting point of the lockdown. The results offer a deep insight into $PM_{2.5}$ source changes and help develop suitable emission control measures.

2 Methodology

2.1 Model description

The State-wide Air Pollution Research Center version 11 (SAPRC-11) photochemical mechanism and AERO6 aerosol module are applied in the CMAQ v5.0.2 to separately quantify source contributions to PPM and SIA (Carter and Heo, 2013; Zhang et al., 2015). The CMAQ model used in this study was modified with additional non-reactive tracers of PPM from various source sectors and regions (Hu et al., 2015). The emission rates of these tracers only account for 0.001 % of total PPM emission rates in each grid cell so that they will not have an impact on the atmospheric process, as shown in Eq. (1) as follows:

$$\mathrm{ATCR}_i = 10^{-5} \cdot \mathrm{PPM}_i, \quad (1)$$

where ATCR_i represents emission rate of the tracer from the ith emission source or region with PPM emission rate of PPM_i, and 10^{-5} is the scaling factor. The concentrations of tracers from a given source or region are then estimated by multiplying 10^5 to represent the concentrations of PPM from that source or region. The concentrations of components in PPM are calculated based on the ratio of each component to total PPM from sources or regions. Details were discussed in Hu et al. (2015).

The contributions of source sectors and regions to SIA are quantified by tagging reactive tracers. Precisely, both the components of SIA and their precursors from diverse source types and regions are tracked separately by adding labels on NO_x, SO_2, and NH_3 through the atmospheric process (Shi et al., 2017). In this study, contributions from different emission sectors, including residential, industrial, transportation, power, and agriculture, and those from source regions, including Jiangsu, Shanghai, Zhejiang, Anhui, HaBTH (Henan, Beijing, Hebei,and Tianjin), Shandong, HnHb (Hunan and Hubei) and other provinces, are tracked (Fig. S1 and Table S1 in the Supplement). The SOA simulation has considerable uncertainties which were caused by the inadequate knowledge of its precursors, incomprehensive formation mechanisms in the model, and limited observations (Zhao et al., 2016; Yang et al., 2019; Heald et al., 2005; Carlton et al., 2008). Therefore, the SOA sources are not tracked in this study. More information on SOA source apportionment was discussed in Wang et al. (2018).

2.2 Model application

A total of two nested domains were used to simulate pollution changes during the COVID-19 pandemic from 5 January to 28 February 2020. As shown in Fig. S1, China and its surrounding areas are covered in the outer 36 km domain (197×127 grid cells), and the YRD is covered by the inner 12 km domain (97×88 grid cells). The first 5 d simulation is removed to minimize the effect of initial conditions. The boundary conditions used in the 12 km domain are offered by the 36 km simulations. Meteorology inputs were generated by the Weather Research and Forecasting (WRF) model v3.6.1. The boundary and initial conditions for WRF were from the National Centers for Environmental Prediction (NCEP) Final (FNL) Operational Model Global Tropospheric Analyses data set (available at http://rda.ucar.edu/datasets/ds083.2/, last access: 10 March 2021). The anthropogenic emissions in China, based on the Multi-resolution Emission Inventory for China (MEIC; http://www.meicmodel.org, last access: 10 March 2021), include industrial, power, agriculture, residential, and transportation. The emissions from other countries were obtained from the Emissions Database for Global Atmospheric Research (EDGAR) v4.3 (http://edgar.jrc.ec.europa.eu/overview.php?v=_431, last access: 6 May 2021). Biogenic emissions were generated using the Model of Emissions of Gases and Aerosols from Nature (MEGAN) v2.1 (Guenther et al., 2012, 2006).

A total of two cases were simulated in this study (Table 1). The base case (case 1) used the original inventory. In case 2, the emissions of carbon monoxide (CO), nitric oxide (NO_x), sulfur dioxide (SO_2), volatile organic compounds (VOC), and PM decreased during the COVID-19 period, since 23 January 2020, with provincial-specific factors as described in Huang et al. (2020). The differences between the cases represent the changes in sources and regions.

3 Results and discussion

3.1 Model performance

3.1.1 WRF evaluation

Since air quality simulations are influenced by meteorological differences, it is critical to validate the WRF performance before simulating source apportionment (Zhang et al., 2015). The model performance of meteorological parameters, including temperature at 2 m above the ground surface ($T2$), wind speed (WSPD), wind direction (WD), and relative humidity (RH), in the COVID-19 period are found in Table S2. The statistical values of mean prediction (PRE), mean observation (OBS), mean bias (MB), gross error (GE), and root mean square error (RMSE) have been calculated, and the calculation formulas are listed in Table S4. $T2$ predicted by the WRF model were slightly higher than observations in the two periods. The MB values of $T2$ before and after the lockdown were both 1.6, while the GE value of $T2$ before the lockdown period was slightly larger than the recommended criterion, based on Emery et al. (2001). Except for the MB values of WSPD, both GE (1.3 and 1.6) and RMSE (1.7 and 2.0) met the benchmarks during the two periods. The MB (1.8) and GE (29.2) values of WD were all within the benchmarks after the lockdown, but the GE value of WD before the lockdown was slightly higher than the benchmark. The simulated RH was underestimated with the MB values of -2.4 and -5.6 during the two periods. The hourly comparisons of $T2$, WSPD, and RH shown in Fig. S9, based on Y. Wang et al. (2020), also indicated good model performance. Compared to previous studies (Chen et al., 2019; Liu et al., 2020), the meteorology predictions in this study were robust enough to drive air quality simulation. Generally, the WRF model in this study showed a good performance, which was comparable to previous study (Shen et al., 2020b; Wang et al., 2021).

3.1.2 CMAQ evaluation

The model performance of O_3, NO_2, SO_2, $PM_{2.5}$, and PM_{10} mass in the YRD during the COVID-19 pandemic has been described in Table S2 of a previous study (Y. Wang et al., 2020b). During the whole simulated period, the predicted $PM_{2.5}$ and O_3 were slightly higher than observations, but the model performance was within the criteria for $PM_{2.5}$ (mean fractional bias – MFB $\leq \pm 60\,\%$; mean fractional error – MFE $\leq 75\,\%$; suggested by Boylan and Russell, 2006) and for O_3 (MFB $\leq \pm 15\,\%$; MFE $\leq 30\,\%$; suggested by U.S. EPA, 2007). Figure 1 shows the predicted and observed daily $PM_{2.5}$ averaged over the YRD and at three major cities, based on case 2 and case 1. Generally, compared to case 1, the lockdown significantly decreases the $PM_{2.5}$ concentration. The temporal trends of $PM_{2.5}$ mass before and during the lockdown were successfully captured by the model simulations. The MFB and MFE values of $PM_{2.5}$ mass were 0.14–0.41 and 0.38–0.57, which were all within the criteria. In Shanghai, the simulations missed the $PM_{2.5}$ episodes from 11 to 13 January, but the overall performance was good. Although overprediction occurred both in case 1 and case 2, the slope of case 2 was closer to the 1 : 1 line, with a higher correction coefficient compared to case 1 (Fig. S3). It indicated that the model performance was better after adjusting the emission. This discrepancy could be caused by the uncertainties in the emissions (Ying et al., 2014). The model simulation of the WRF was the same in the two cases. The 2016 MEIC emission was used for the year 2020, which might overestimate the anthropogenic emissions and, thus, the $PM_{2.5}$ concentration in the before-lockdown period. However, the emission adjustments based on Huang et al. (2020) during lockdown may be closer to the real condition, leading to better model performance. In addition, observed SIA (including sulfate, nitrate, and ammonium) from 8 January to 10 February 2020 in Shanghai, reported by Chen

Table 1. Simulation scenarios during the COVID-19 period in this study, based on Huang et al. (2020).

	Province	CO	NO_x	SO_2	VOC	$PM_{2.5}$	BC	OC
Case 1	All	No changes						
Case 2	Beijing	22 %	45 %	26 %	45 %	18 %	46 %	8 %
	Tianjin	21 %	38 %	20 %	41 %	14 %	22 %	6 %
	Hebei	15 %	45 %	16 %	36 %	12 %	17 %	5 %
	Shanxi	18 %	40 %	20 %	33 %	16 %	19 %	10 %
	Inner Mongolia	14 %	29 %	15 %	34 %	13 %	16 %	6 %
	Liaoning	21 %	40 %	28 %	36 %	16 %	28 %	8 %
	Jilin	16 %	39 %	23 %	34 %	13 %	18 %	5 %
	Heilongjiang	17 %	37 %	27 %	28 %	13 %	15 %	7 %
	Shanghai	35 %	48 %	42 %	45 %	34 %	54 %	42 %
	Jiangsu	23 %	50 %	26 %	41 %	16 %	35 %	7 %
	Zhejiang	41 %	50 %	29 %	45 %	30 %	49 %	20 %
	Anhui	14 %	56 %	22 %	31 %	11 %	22 %	4 %
	Fujian	29 %	51 %	30 %	42 %	19 %	31 %	7 %
	Jiangxi	24 %	53 %	21 %	43 %	19 %	30 %	9 %
	Shandong	23 %	50 %	25 %	39 %	19 %	35 %	9 %
	Henan	23 %	57 %	22 %	41 %	18 %	35 %	8 %
	Hubei	19 %	55 %	23 %	35 %	16 %	23 %	10 %
	Hunan	22 %	51 %	25 %	36 %	20 %	24 %	15 %
	Guangdong	38 %	50 %	33 %	46 %	27 %	42 %	13 %
	Guangxi	24 %	50 %	28 %	39 %	17 %	27 %	5 %
	Hainan	24 %	44 %	25 %	36 %	14 %	25 %	4 %
	Chongqing	18 %	53 %	32 %	37 %	14 %	20 %	4 %
	Sichuan	16 %	50 %	27 %	33 %	9 %	15 %	3 %
	Guizhou	24 %	39 %	25 %	30 %	22 %	25 %	20 %
	Yunnan	24 %	51 %	25 %	41 %	18 %	21 %	8 %
	Tibet	16 %	35 %	15 %	35 %	14 %	14 %	5 %
	Shaanxi	19 %	45 %	18 %	34 %	13 %	22 %	5 %
	Gansu	13 %	47 %	16 %	29 %	9 %	13 %	3 %
	Qinghai	23 %	46 %	22 %	39 %	20 %	20 %	7 %
	Ningxia	24 %	36 %	24 %	39 %	20 %	23 %	8 %
	Xinjiang	16 %	35 %	15 %	35 %	14 %	14 %	5 %

et al. (2020), was used to evaluate the model performance, as shown in Fig. S4. The daily simulated trends of SIA generally agreed with the observations, although the model slightly overpredicted SIA concentrations, with MFB values of 0.19–0.37 and MFE values of 0.41–0.68 (Table S3). The overestimation of nitrate has been reported in the previous studies (Chang et al., 2018; Shen et al., 2020b; Choi et al., 2019), and the possible reason was the lack of chlorine heterogeneous chemistry in the model (Qiu et al., 2019). Despite these uncertainties, the model results were acceptable for source apportionment studies.

3.2 Changes in $PM_{2.5}$ and components during the lockdown

Figure 2 shows the predicted total $PM_{2.5}$ and its components in the YRD during the COVID-19 lockdown. In both cases, $PM_{2.5}$ and its components showed similar spatial distributions, with the highest concentrations in the northwest and lower concentrations in the southeast. Substantial $PM_{2.5}$ was observed in north Anhui, and similar patterns were found in elemental carbon (EC) and primary organic aerosol (POA), indicating similar sources and large contributions. For case 2, averaged $PM_{2.5}$ concentrations mainly decreased in the northern and western YRD, due to the lockdown, and all major components decreased in varying degrees. For EC and POA, similar decreases of 15 % were observed in Anhui, compared to case 1. More significant decreases were found in other regions, especially in Zhejiang (up to 25 %). SIA had the maximum decrease in Anhui (30 %–40 %), which was related to sharp drops in concentrations in nitrate and ammonium, with decreases of 40 %–50 % and 30 %–40 % (Fig. S5), respectively. On the contrary, the reductions in sulfate in Shanghai were higher than other regions in the YRD, mainly due to a greater reduction in SO_2 from industries during the lockdown, based on Huang et al. (2020). Except for central and northwestern YRD, SOA decreased significantly (35 %–40 %), also due to the reductions in industrial activi-

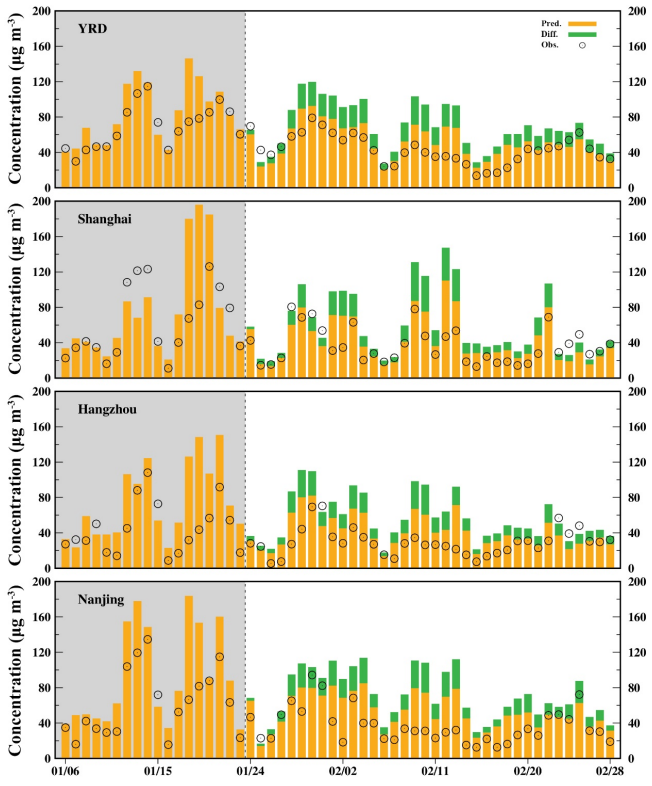

Figure 1. Predicted daily $PM_{2.5}$, with observed daily $PM_{2.5}$, in the YRD, and three major cities in case 2 (orange histogram) before (shaded area) and during (white area) the lockdown period. The green histogram (Diff.) represents the concentration difference in $PM_{2.5}$, which is calculated as case 1 − case 2. Units are in micron grams per cubic meter ($\mu g\,m^{-3}$). Pred. is the predicted $PM_{2.5}$ concentration, and Obs. is the observed $PM_{2.5}$ concentration.

ties, which was an important contributor to SOA (Liu et al., 2020).

Figure 3 shows the contributions of components to $PM_{2.5}$ in the YRD and three major cities during the lockdown. For case 2, over the entire YRD, the reductions in POA, EC, sulfate, nitrate, ammonium, and SOA were 2.4, 0.8, 2.1, 7.8, 2.9, and 0.9 $\mu g\,m^{-3}$, with a total of 17.0 $\mu g\,m^{-3}$ decrease in $PM_{2.5}$. The most significant percent decrease was found in nitrate, with the highest decrease rate of over 40 %. In selected cities, $PM_{2.5}$ decreased by 15.1, 14.8, and 16.8 $\mu g\,m^{-3}$ in Shanghai, Hangzhou, and Nanjing, respectively, with the largest percent decrease of 27 % in Hangzhou. Secondary components (SIA and SOA) dropped more significantly than primary components, especially for nitrate (35 %–45 %) due to the severe decrease in NO_x from transportation. This also indicated that atmospheric reactions were important during the lockdown period. In addition to nitrate, a sharp decrease was observed in ammonium due to the decrease in both nitrate and sulfate (Erisman and Schaap, 2004). SIA concentrations contributed the most to $PM_{2.5}$ in selected cities, with the highest values of 26.5 $\mu g\,m^{-3}$ in Nanjing. Furthermore, the largest contributor to SIA was nitrate in the YRD, Hangzhou, and Nanjing during the lockdown, while sulfate became the dominant contributor in Shanghai and accounted for 22 % of total $PM_{2.5}$, similar to the result in Chen et al. (2020).

With the impact of the lockdown, the $PM_{2.5}$ concentrations decreased significantly in the YRD region, mainly due to the reduction in the concentration of PPM and SIA. The results provided a solid basis for conducting the source apportionment of the $PM_{2.5}$ components. And the next section shows the source apportionment and regional transport of $PM_{2.5}$.

3.3 Source sector contributions to $PM_{2.5}$

Figure 4 shows the contributions of different source sectors to $PM_{2.5}$ in the YRD during the lockdown. Source apportionments of SIA and PPM in two cases are illustrated in Figs. S6 and S8, respectively. The agricultural source of PPM is not shown due to minor contributions. Generally, residential activities were the most significant contributor to $PM_{2.5}$, with the highest value of 45.0 $\mu g\,m^{-3}$ mainly due to the large contribution to PPM (Fig. S8). The contribution in Shanghai was $\sim$ 20.0 $\mu g\,m^{-3}$, and it decreased to 15.0 $\mu g\,m^{-3}$ during the lockdown. The overall decrease was less than 10 % in the middle YRD and less than 15 % in the rest of the regions. Contributions from transportation decreased the most due to the lockdown, from larger than 10.0 $\mu g\,m^{-3}$ in case 1 to less than 7.5 $\mu g\,m^{-3}$, in most areas. This is shown in SIA as well (Fig. S6), where over 40 % decreases were found in the YRD, except for the southeast, with the maximum decrease value of $\sim$ 7.0 $\mu g\,m^{-3}$. The industry contributed the most to $PM_{2.5}$ values in industrial cities such as Suzhou and Hefei (positions as shown in Fig. S1), which decreased significantly by $\sim$ 10.0 $\mu g\,m^{-3}$, from $>$ 30.0 to $\sim$ 20.0 $\mu g\,m^{-3}$ in case 2. $PM_{2.5}$ from the power sector decreased by less than 5 % to less than 6 $\mu g\,m^{-3}$ in most areas due to reduced emissions of SO_2 and associated sulfate (Fig. S7). $PM_{2.5}$ from agriculture also decreased during the lockdown, with the largest decrease of 5.0 $\mu g\,m^{-3}$ in the northwestern YRD.

Figure 5 shows the changes in contributions of sources to $PM_{2.5}$ in the YRD, Shanghai, Hangzhou, and Nanjing caused by the lockdown. Overall, in the YRD, residential and industrial sources were major sources, with contributions of 35 % and 33 % and decreases of less than 20 %. Transportation, power, and agriculture sources contributed similarly to $PM_{2.5}$ but with different changing ratios of 40 %, 6 %, and 17 %, respectively. Although all sources decreased, the relative contribution did not remain unchanged. The contribution ratio of transportation decreased by 27 % due to the decrease in both primary emission and secondary formation, as shown in Figs. S9 and S10. The contribution ratios of residential and power increased by more than 10 %, while industry and agriculture showed slight changes. In large cities, industrial sources were leading with 5.0–10.0 $\mu g\,m^{-3}$ higher contribution than residential sources, while other sources were similar to the YRD averages. In Shanghai, the contributions of

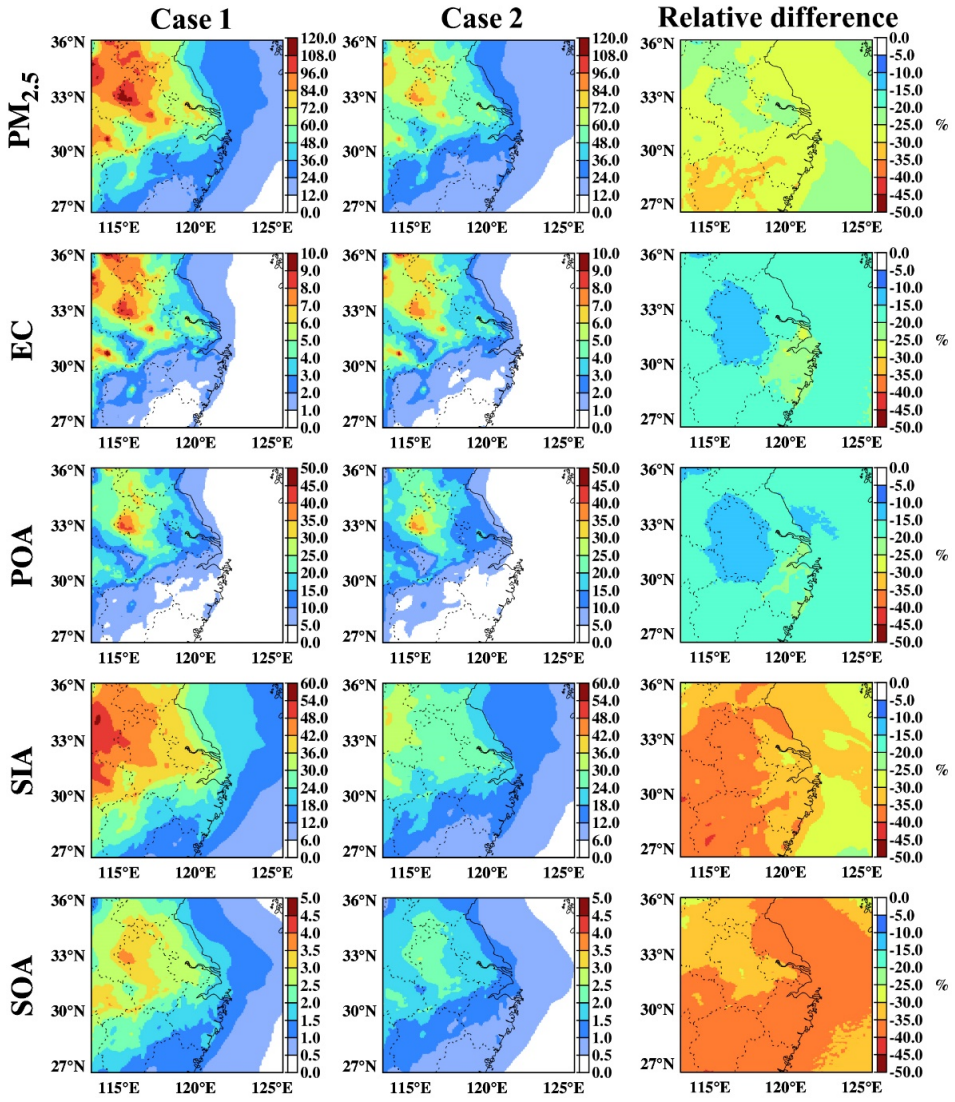

Figure 2. Spatial distribution of predicted $PM_{2.5}$ total and major components and changes caused by the lockdown measures in the YRD from 23 January to 28 February 2020. EC is elemental carbon, and POA is primary organic aerosol. The relative difference is calculated as (case 2 − case 1)/case 1, using the concentration. Note that the color ranges are different among panels.

power and agriculture showed insignificant changes, while that of the industry changed by ∼ 20 %, and transportation decreased by more than 30 %. The relative contribution of transportation decreased by more than 15 %, while that of power and agriculture increased by 14 % and 9 %, respectively. In Hangzhou and Nanjing, the trends were similar, except that the contributions of and changes in all sources were larger in Nanjing. Due to the lockdown measures, contributions of different sources decreased, but their relative contribution changed differently, implying that an adjustment of control measures for various sources is needed.

3.4 Regional contributions to $PM_{2.5}$

Figure 6 illustrates the distribution of $PM_{2.5}$ contributed by emissions from different regions for two cases in the YRD during the lockdown. Regional transmissions of SIA and PPM are shown in Figs. S11 and S12, respectively. It was clear that the regional distributions of each source were the same in both cases, but case 2 had lower values and narrower distributions. Contributions of local emissions from Jiangsu, Shanghai, Zhejiang, and Anhui generally peaked near the source regions, with less than 5.0 $\mu g\,m^{-3}$ transported to other areas. Emissions from HnHb were barely transported to the central YRD area. Shandong and Ha-BTH emissions could be transported further due to northerly winds, as shown in Fig. S2, with ∼ 10.0 $\mu g\,m^{-3}$ and ∼ 5.0 $\mu g\,m^{-3}$ contributions

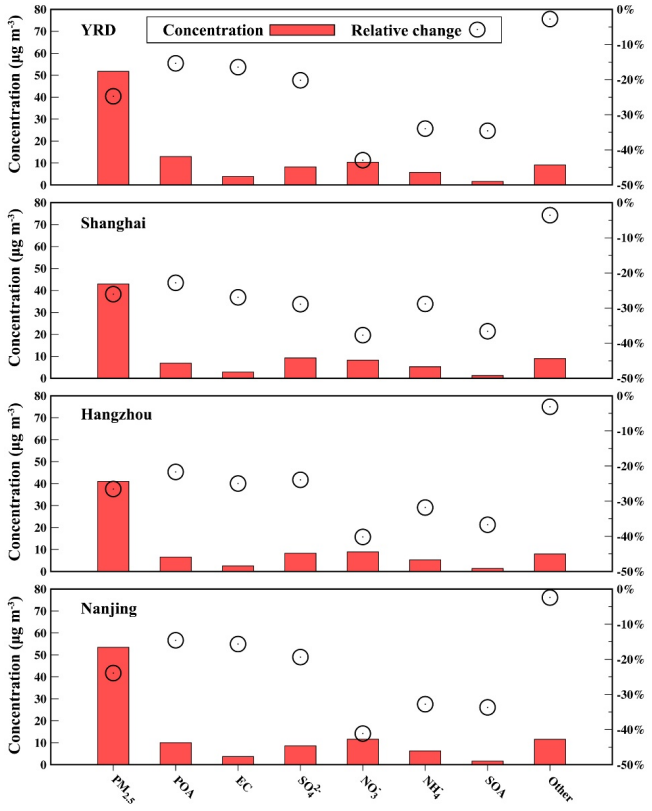

Figure 3. Predicted $PM_{2.5}$ and its major components in case 2 (red histogram corresponding to left y axis) and the relative change (circle corresponding to right y axis) from 23 January to 28 February 2020 in the YRD and Shanghai, Hangzhou, and Nanjing. Here the relative change means the relative change in concentration between case 1 and case 2, which is calculated as (case 2 − case 1)/case 1.

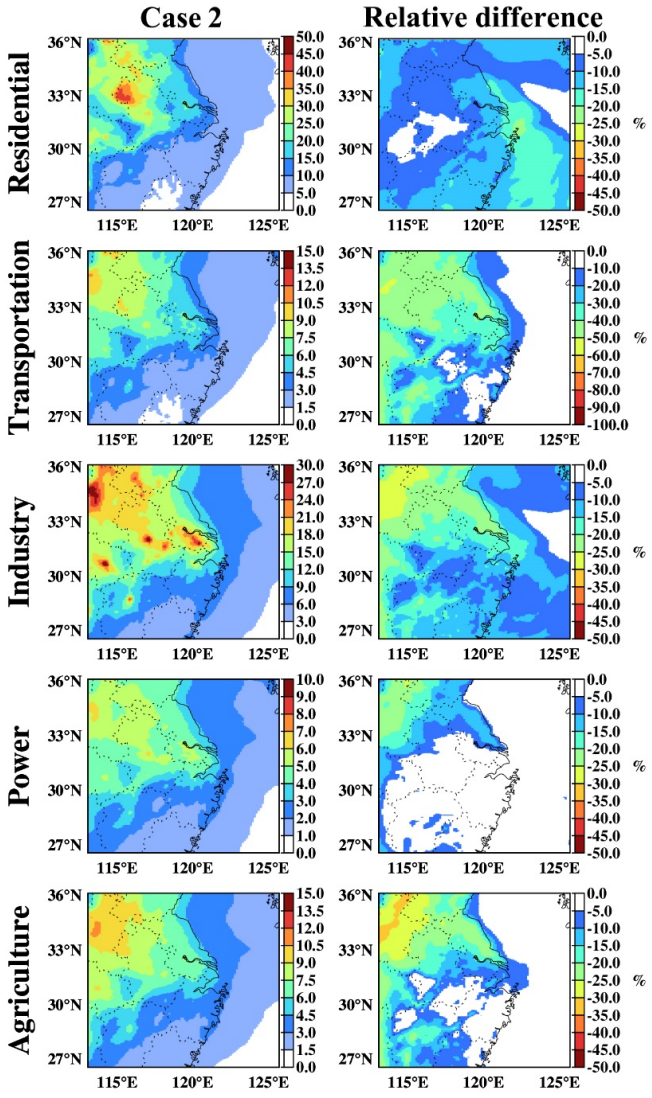

Figure 4. Predicted $PM_{2.5}$ from different source sectors of two cases, and the relative difference in the YRD from 23 January to 28 February 2020. Note that the color ranges are different among panels.

to the northern YRD, respectively. It indicated that the regional transport among provinces was notable, which is consistent with Du et al. (2017). Consequently, the government should strengthen regional joint preventions in addition to local emission reductions. Other regions also had small contributions to the YRD, but the contributions decreased significantly during the lockdown. The limitation of commercial activities and traffic caused by the lockdown significantly decreased the emission of $PM_{2.5}$ and indirectly suppressed its dispersion. Compared to case 1, contributions from Jiangsu, Anhui, Shandong, and Ha-BTH in case 2 decreased by 20 %–30 %. More significant decreases of 30 %–40 % were found in Shanghai, Zhejiang, and HnHb. The largest decrease of $\sim 18.0\,\mu g\,m^{-3}$ was observed in Hubei, the center of the COVID-19 pandemic in China due to stricter lockdown measures. Figure S9 shows that, after the implementation of quarantine measures, the SIA contributions decreased by more than 30 % among each region, and HnHb decreased by 51 % to less than $10.0\,\mu g\,m^{-3}$. Figure S10 shows the narrower distributions and smaller decreases in PPM in case 2 compared with SIA, with a decrease of less than 30 % in all selected regions.

Figure 7 illustrates the average $PM_{2.5}$ contributed by eight regions in the YRD and Shanghai. In the YRD, averaged contributions due to local emissions from Jiangsu, Shanghai, Zhejiang, and Anhui were 6.8, 0.8, 1.5, and $6.3\,\mu g\,m^{-3}$ during the lockdown period, while the contribution of areas outside YRD, from HnHb, Shandong, Ha-BTH, and others, were 5.0, 9.1, 14.4, and $8.2\,\mu g\,m^{-3}$, respectively. The contributions of all regions decreased due to the COVID-19 lockdown, with the averaged decrease of 20 %–30 %, the largest decrease of 33 % in HnHb, and the least decrease of 21 % in Jiangsu. In addition to the absolute contributions, Fig. 7b also shows the relative contribution of different regions. Ha-

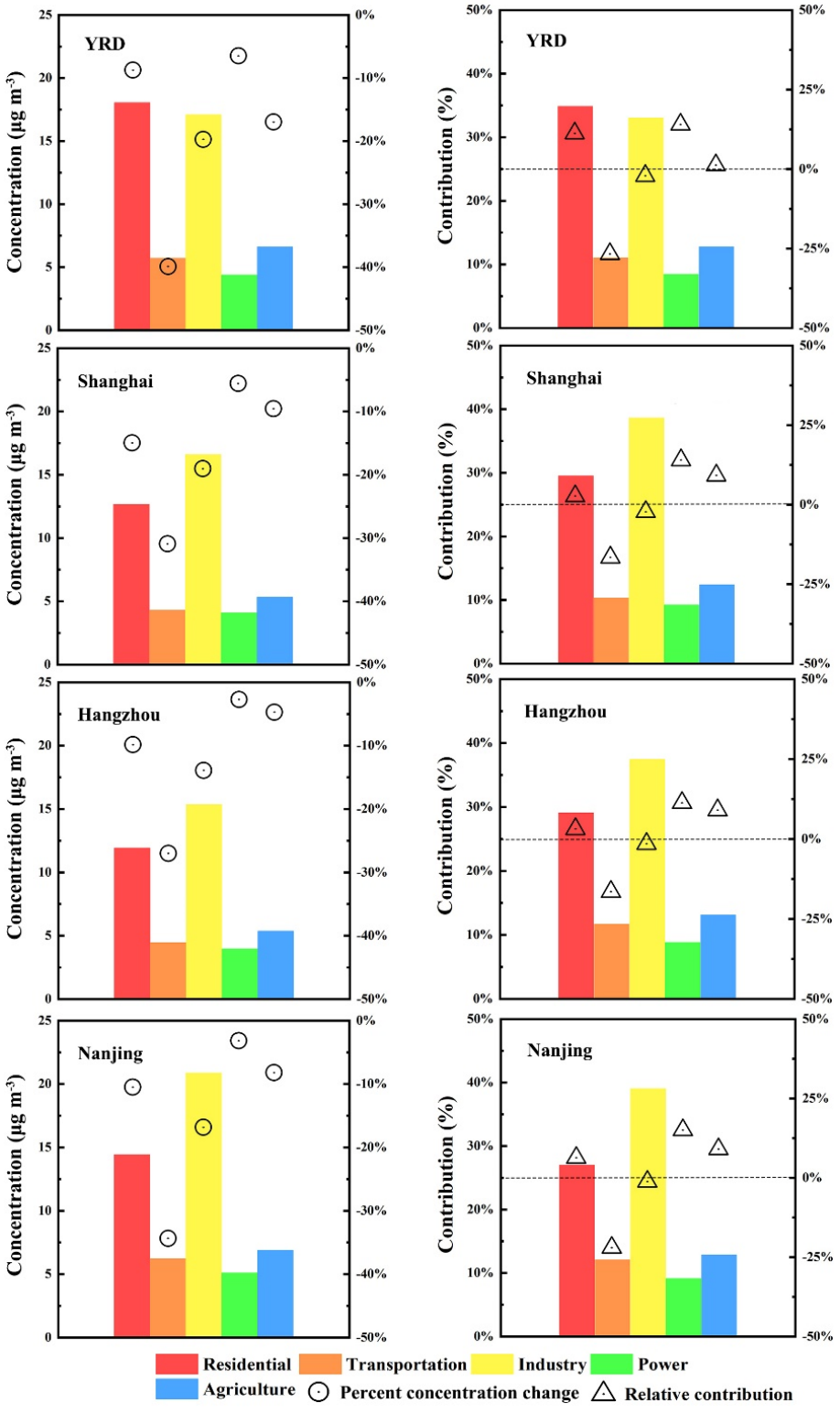

Figure 5. Concentrations and contributions of different emission sectors to $PM_{2.5}$ in the YRD and three major cities in case 2 from 23 January to 28 February 2020. The values of the histograms correspond to the left y axis and the values of relative changes correspond to the right y axis. The relative contribution means the relative change in contribution between case 1 and case 2, calculated as (case 2 − case 1)/case 1. The percent concentration change means the relative change in concentration, calculated as (case 2 − case 1)/case 1.

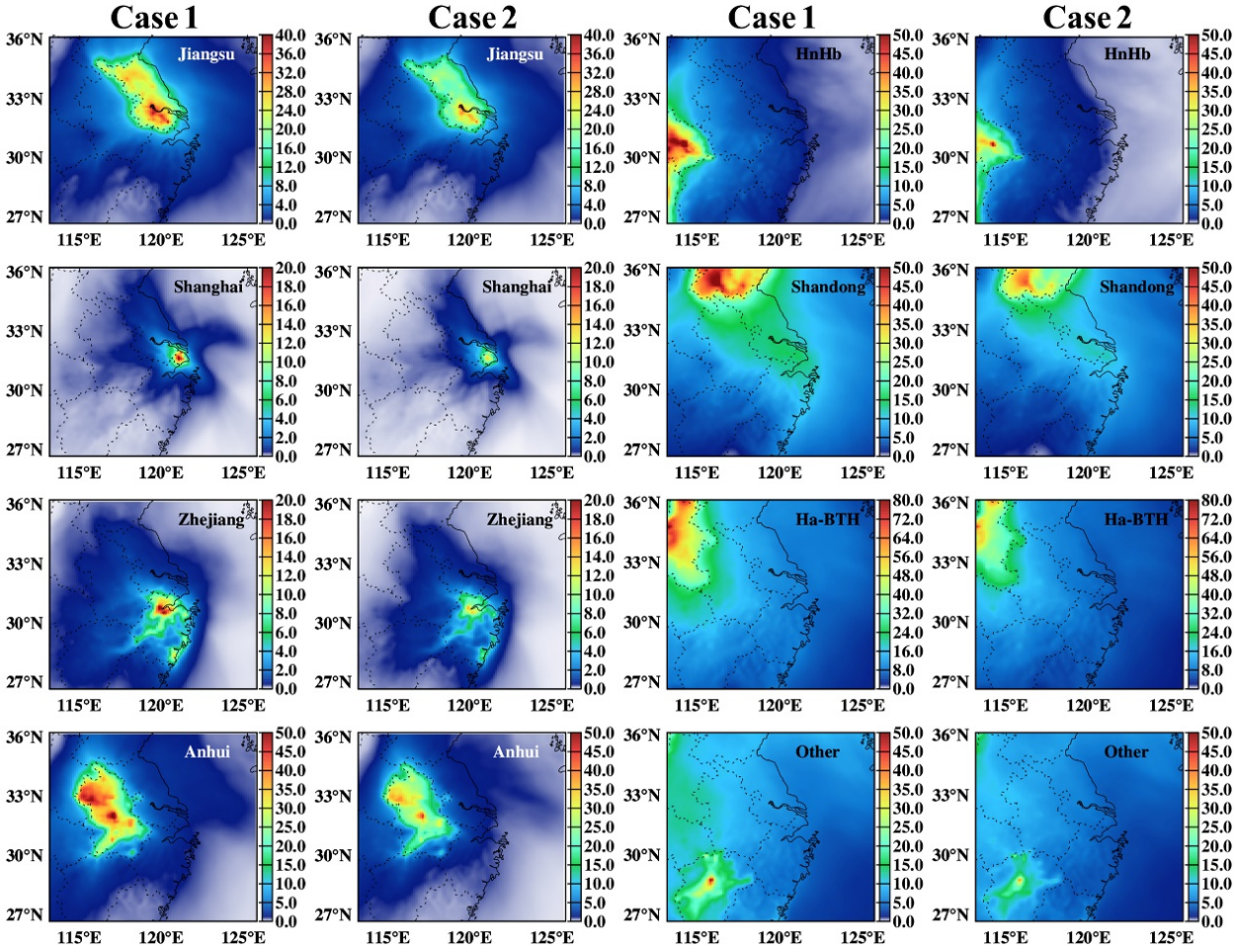

Figure 6. Averaged regional contributions of predicted $PM_{2.5}$ in the YRD from 23 to 28 February 2020. Note that the color ranges are different among panels.

BTH had the largest contribution of ∼ 30 %, followed by Shandong and others. Jiangsu and Anhui were the largest local contributors, with ∼ 12 % each. It is clear that long-range transport played an important role in $PM_{2.5}$ pollution in the YRD with a contribution of more than 70 %. Due to the COVID-19, although the absolute contributions decreased universally, their relative contributions did not. The importance of Jiangsu and Shandong increased by ∼ 5 %, while that of Shanghai, Zhejiang, and HnHb decreased with the largest rate of 12 % in HnHb. The results showed that, although all regions reduced their concentrations to the YRD, the relative contribution changed. In the future, regional cooperative control is needed for the YRD, and strategies should be adjusted according to changes in contributions.

At the city level, local emissions were the major contributor, with contributions of 10.0 $\mu g\,m^{-3}$ within the YRD to Shanghai, the largest city in the YRD (Fig. 7c). Jiangsu contributed 16 % to Shanghai, while Zhejiang and Anhui had few effects. Outside the YRD, Shandong had the largest contribution (11.5 $\mu g\,m^{-3}$), followed by Ha-BTH and other areas. In total, contributions from neighboring provinces ($< 10.0\,\mu g\,m^{-3}$) were much smaller than long-range transport from outside the YRD (23.7 $\mu g\,m^{-3}$). Prevailing northerly winds were a key factor in this instance (Fig. S2). The lockdown decreased the contributions from all regions by 20 %–45 %, with the largest decrease from HnHb. The contribution order of different regions was unchanged, but their relative contributions changed. The relative contributions of local emissions from Shanghai decreased by ∼ 10 %, while that of Shandong and Jiangsu increased by ∼ 10 %. The relative contribution of HnHb decreased by more than 20 %, although the absolute changes were small.

The quarantine measures during the COVID-19 lockdown reduced emissions from transportation and industry, and the total emissions for different areas changed differently. Although $PM_{2.5}$ concentrations decreased in the whole YRD, the contributions of source sectors and regions changed differently. It highlighted the need for regional cooperative emission reduction and adjustment of the control strategies when significant reductions were achieved.

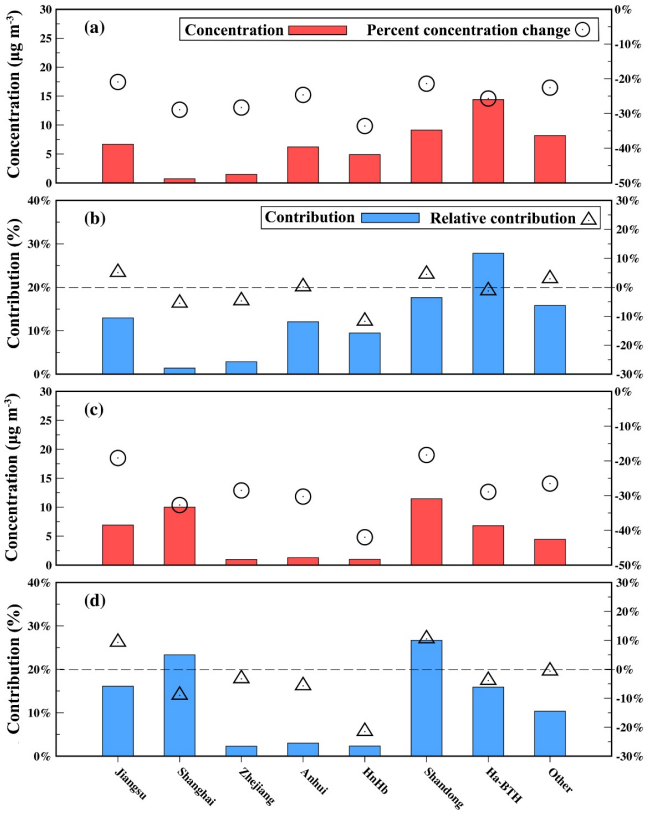

Figure 7. Concentrations and contributions of predicted $PM_{2.5}$ from different regions in the YRD **(a, b)** and Shanghai **(c, d)** of case 2, corresponding to the left *y* axis and the relative change (corresponding to the right *y* axis) from 23 January to 28 February 2020. The meanings of relative contribution and percent concentration change are the same as in Fig. 5.

4 Conclusions

A source-oriented CMAQ model investigated the changes in contributions of source sectors and regions to $PM_{2.5}$ during the COVID-19 lockdown in the YRD. Total $PM_{2.5}$ mass decreased by more than 20 % across the YRD due to decreases of 30 %–40 % and 10 %–20 % in secondary and primary components, respectively. The results of the source apportionment showed that the residential and industrial sources were the major sources, with contributions of 35 % (18.0 $\mu g\,m^{-3}$) and 33 % (17.1 $\mu g\,m^{-3}$), decreasing by less than 20 % due to the lockdown. Contributions from transportation decreased by 40 %, which was the most significant decrease, while the decrease in power was less than 10 %. The relative contribution of sources changed due to differences in source decreases. The relative contribution of transportation decreased by more than 25 %, while that of residential and power increased by more than 10 %, suggesting that further abatement policies should adjust control measures for various sources. Contributions from the regional transport of emissions outside the YRD were the dominant contributors (more than 70 %) to the YRD, and contributions from all regions decreased due to the lockdown. The relative contribution of each region also changed, with increases in Jiangsu and Shandong (∼ 10 %) but decreases in all other regions. This implied that strengthening the regional joint preventions and control of transported pollution from heavily polluted regions could effectively mitigate $PM_{2.5}$ pollution in the YRD.

Code availability. CMAQ model code is available from the United States Environmental Protection Agency (https://www.epa.gov/cmaq/access-cmaq-source-code, last access: 6 May 2021, Simon and Bhave, 2012), and the WRF model code is available from the WRF user page (https://www2.mmm.ucar.edu/wrf/users/download/get_sources.html, last access: 6 May 2021, Skamarock et al., 2008).

Data availability. Data used in this paper can be obtained upon request from the corresponding author (zhanghl@fudan.edu.cn).

Supplement. The supplement related to this article is available online at: https://doi.org/10.5194/acp-21-7343-2021-supplement.

Author contributions. JM conducted the modeling and led the writing, with writing assistance from JS. PengW, SZ, YW and PengfW collected data and provided technical support. GW assisted with data analysis. JC and HZ designed the study, discussed the results, and edited the paper.

Competing interests. The authors declare that they have no conflict of interest.

Acknowledgements. We acknowledge the publicly available WRF and CMAQ models that made this study possible.

Financial support. This research was funded by the Institute of Eco-Chongming (grant no. ECNU-IEC-202001).

Review statement. This paper was edited by Thomas Karl and reviewed by two anonymous referees.

References

Boylan, J. W. and Russell, A. G.: PM and light extinction model performance metrics, goals, and criteria for three-dimensional air quality models, Atmos. Environ., 40, 4946–4959, https://doi.org/10.1016/j.atmosenv.2005.09.087, 2006.

Cai, S., Wang, Y., Zhao, B., Wang, S., Chang, X., and Hao, J.: The impact of the "Air Pollution Prevention and Control Action Plan" on $PM_{2.5}$ concentrations in Jing-Jin-Ji re-

gion during 2012–2020, Sci. Total Environ., 580, 197–209, https://doi.org/10.1016/j.scitotenv.2016.11.188, 2017.

Carlton, A. G., Turpin, B. J., Altieri, K. E., Seitzinger, S. P., Mathur, R., Roselle, S. J., and Weber, R. J.: CMAQ Model Performance Enhanced When In-Cloud Secondary Organic Aerosol is Included: Comparisons of Organic Carbon Predictions with Measurements, Environ. Sci. Technol., 42, 8798–8802, https://doi.org/10.1021/es801192n, 2008.

Carter, W. P. L. and Heo, G.: Development of revised SAPRC aromatics mechanisms, Atmos. Environ., 77, 404–414, https://doi.org/10.1016/j.atmosenv.2013.05.021, 2013.

Chang, X., Wang, S., Zhao, B., Cai, S., and Hao, J.: Assessment of inter-city transport of particulate matter in the Beijing–Tianjin–Hebei region, Atmos. Chem. Phys., 18, 4843–4858, https://doi.org/10.5194/acp-18-4843-2018, 2018.

Chauhan, A. and Singh, R. P.: Decline in $PM_{2.5}$ concentrations over major cities around the world associated with COVID-19, Environ. Res., 187, 109634, https://doi.org/10.1016/j.envres.2020.109634, 2020.

Chen, D., Tian, X., Lang, J., Zhou, Y., Li, Y., Guo, X., Wang, W., and Liu, B.: The impact of ship emissions on $PM_{2.5}$ and the deposition of nitrogen and sulfur in Yangtze River Delta, China, Sci. Total Environ., 649, 1609–1619, https://doi.org/10.1016/j.scitotenv.2018.08.313, 2019.

Chen, H., Huo, J., Fu, Q., Duan, Y., Xiao, H., and Chen, J.: Impact of quarantine measures on chemical compositions of $PM_{2.5}$ during the COVID-19 epidemic in Shanghai, China, Sci. Total Environ., 743, 140758, https://doi.org/10.1016/j.scitotenv.2020.140758, 2020.

China: Air quality targets set by the Action Plan have been fully realized, available at: http://www.gov.cn/xinwen/2018-02/01/content_5262720.htm/, last access: 1 Febuary 2018.

Choi, M.-W., Lee, J.-H., Woo, J.-W., Kim, C.-H., and Lee, S.-H.: Comparison of $PM_{2.5}$ Chemical Components over East Asia Simulated by the WRF-Chem and WRF/CMAQ Models: On the Models' Prediction Inconsistency, Atmosphere, 10, 618, https://doi.org/10.3390/atmos10100618, 2019.

Du, W., Hong, Y., Xiao, H., Zhang, Y., Chen, Y., Xu, L., Chen, J., and Deng, J.: Chemical Characterization and Source Apportionment of $PM_{2.5}$ during Spring and Winter in the Yangtze River Delta, China, Aerosol Air Qual. Res., 17, 2165–2180, https://doi.org/10.4209/aaqr.2017.03.0108, 2017.

Du, Y. and Li, T.: Assessment of health-based economic costs linked to fine particulate ($PM_{2.5}$) pollution: a case study of haze during January 2013 in Beijing, China, Air Qual. Atmos. Hlth., 9, 439–445, https://doi.org/10.1007/s11869-015-0387-7, 2016.

Emery, C., Tai, E., and Yarwood, G.: Enhanced meteorological modeling and performance evaluation for two Texas episodes. Report to the Texas Natural Resources Conservation Commission, p.b.E., International Corp, Novato, CA, 2001.

Erisman, J. W. and Schaap, M.: The need for ammonia abatement with respect to secondary PM reductions in Europe, Environ. Pollut., 129, 159–163, https://doi.org/10.1016/j.envpol.2003.08.042, 2004.

Gao, J., Peng, X., Chen, G., Xu, J., Shi, G.-L., Zhang, Y.-C., and Feng, Y.-C.: Insights into the chemical characterization and sources of $PM_{2.5}$ in Beijing at a 1-h time resolution, Sci. Total Environ., 542, 162–171, https://doi.org/10.1016/j.scitotenv.2015.10.082, 2016.

Guenther, A., Karl, T., Harley, P., Wiedinmyer, C., Palmer, P. I., and Geron, C.: Estimates of global terrestrial isoprene emissions using MEGAN (Model of Emissions of Gases and Aerosols from Nature), Atmos. Chem. Phys., 6, 3181–3210, https://doi.org/10.5194/acp-6-3181-2006, 2006.

Guenther, A. B., Jiang, X., Heald, C. L., Sakulyanontvittaya, T., Duhl, T., Emmons, L. K., and Wang, X.: The Model of Emissions of Gases and Aerosols from Nature version 2.1 (MEGAN2.1): an extended and updated framework for modeling biogenic emissions, Geosci. Model Dev., 5, 1471–1492, https://doi.org/10.5194/gmd-5-1471-2012, 2012.

He, J. and Christakos, G.: Space-time $PM_{2.5}$ mapping in the severe haze region of Jing-Jin-Ji (China) using a synthetic approach, Environ. Pollut., 240, 319–329, https://doi.org/10.1016/j.envpol.2018.04.092, 2018.

Heald, C. L., Jacob, D. J., Park, R. J., Russell, L. M., Huebert, B. J., Seinfeld, J. H., Liao, H., and Weber, R. J.: A large organic aerosol source in the free troposphere missing from current models, Geophys. Res. Lett., 32, L18809, https://doi.org/10.1029/2005gl023831, 2005.

Hu, J., Wu, L., Zheng, B., Zhang, Q., He, K., Chang, Q., Li, X., Yang, F., Ying, Q., and Zhang, H.: Source contributions and regional transport of primary particulate matter in China, Environ. Pollut., 207, 31–42, https://doi.org/10.1016/j.envpol.2015.08.037, 2015.

Huang, R.-J., Zhang, Y., Bozzetti, C., Ho, K.-F., Cao, J.-J., Han, Y., Daellenbach, K. R., Slowik, J. G., Platt, S. M., Canonaco, F., Zotter, P., Wolf, R., Pieber, S. M., Bruns, E. A., Crippa, M., Ciarelli, G., Piazzalunga, A., Schwikowski, M., Abbaszade, G., Schnelle-Kreis, J., Zimmermann, R., An, Z., Szidat, S., Baltensperger, U., Haddad, I. E., and Prévôt, A. S. H.: High secondary aerosol contribution to particulate pollution during haze events in China, Nature, 514, 218–222, https://doi.org/10.1038/nature13774, 2014.

Huang, X., Ding, A., Gao, J., Zheng, B., Zhou, D., Qi, X., Tang, R., Wang, J., Ren, C., Nie, W., Chi, X., Xu, Z., Chen, L., Li, Y., Che, F., Pang, N., Wang, H., Tong, D., Qin, W., Cheng, W., Liu, W., Fu, Q., Liu, B., Chai, F., Davis, S. J., Zhang, Q., and He, K.: Enhanced secondary pollution offset reduction of primary emissions during COVID-19 lockdown in China, Natl. Sci. Rev., 8, nwaa137, https://doi.org/10.1093/nsr/nwaa137, 2020.

Lelieveld, J., Evans, J. S., Fnais, M., Giannadaki, D., and Pozzer, A.: The contribution of outdoor air pollution sources to premature mortality on a global scale, Nature, 525, 367–371, https://doi.org/10.1038/nature15371, 2015.

Li, L., Li, Q., Huang, L., Wang, Q., Zhu, A., Xu, J., Liu, Z., Li, H., Shi, L., Li, R., Azari, M., Wang, Y., Zhang, X., Liu, Z., Zhu, Y., Zhang, K., Xue, S., Ooi, M. C. G., Zhang, D., and Chan, A.: Air quality changes during the COVID-19 lockdown over the Yangtze River Delta Region: An insight into the impact of human activity pattern changes on air pollution variation, Sci. Total Environ., 732, 139282, https://doi.org/10.1016/j.scitotenv.2020.139282, 2020.

Liu, J., Shen, J., Cheng, Z., Wang, P., Ying, Q., Zhao, Q., Zhang, Y., Zhao, Y., and Fu, Q.: Source apportionment and regional transport of anthropogenic secondary organic aerosol during winter pollution periods in the Yangtze River Delta, China, Sci. Total. Environ., 710, 135620, https://doi.org/10.1016/j.scitotenv.2019.135620, 2020.

Liu, Q., Baumgartner, J., Zhang, Y., and Schauer, J. J.: Source apportionment of Beijing air pollution during a severe winter haze event and associated pro-inflammatory responses in lung epithelial cells, Atmos. Environ., 126, 28–35, https://doi.org/10.1016/j.atmosenv.2015.11.031, 2016.

Qiu, X., Ying, Q., Wang, S., Duan, L., Zhao, J., Xing, J., Ding, D., Sun, Y., Liu, B., Shi, A., Yan, X., Xu, Q., and Hao, J.: Modeling the impact of heterogeneous reactions of chlorine on summertime nitrate formation in Beijing, China, Atmos. Chem. Phys., 19, 6737–6747, https://doi.org/10.5194/acp-19-6737-2019, 2019.

Shang, X., Zhang, K., Meng, F., Wang, S., Lee, M., Suh, I., Kim, D., Jeon, K., Park, H., Wang, X., and Zhao, Y.: Characteristics and source apportionment of fine haze aerosol in Beijing during the winter of 2013, Atmos. Chem. Phys., 18, 2573–2584, https://doi.org/10.5194/acp-18-2573-2018, 2018.

Shen, J., Zhao, Q., Cheng, Z., Huo, J., Zhu, W., Zhang, Y., Duan, Y., Wang, X., Antony Chen, L. W., and Fu, Q.: Evolution of source contributions during heavy fine particulate matter ($PM_{2.5}$) pollution episodes in eastern China through online measurements, Atmos. Environ., 232, 117569, https://doi.org/10.1016/j.atmosenv.2020.117569, 2020a.

Shen, J., Zhao, Q., Cheng, Z., Wang, P., Ying, Q., Liu, J., Duan, Y., and Fu, Q.: Insights into source origins and formation mechanisms of nitrate during winter haze episodes in the Yangtze River Delta, Sci. Total Environ., 741, 140187, https://doi.org/10.1016/j.scitotenv.2020.140187, 2020b.

Shi, Z., Li, J., Huang, L., Wang, P., Wu, L., Ying, Q., Zhang, H., Lu, L., Liu, X., Liao, H., and Hu, J.: Source apportionment of fine particulate matter in China in 2013 using a source-oriented chemical transport model, Sci. Total Environ., 601–602, 1476–1487, https://doi.org/10.1016/j.scitotenv.2017.06.019, 2017.

Simon, H., and Bhave, P. V.: Simulating the degree of oxidation in atmospheric organic particles, Environ. Sci. Technol., 46, 331–339, https://doi.org/10.1021/es202361w, 2012.

Skamarock, W. C., Klemp, J. B., Dudhia, J., Gill, D. O., Barker, D. M., Duda, M. G., Huang, X.-Y., Wang, W., and Powers, J. G.: A Description of the Advanced Research WRF Version 3, NCAR Tech. Note NCAR/TN-475+STR, 113 pp., https://doi.org/10.5065/D68S4MVH, 2008.

Song, C., Wu, L., Xie, Y., He, J., Chen, X., Wang, T., Lin, Y., Jin, T., Wang, A., Liu, Y., Dai, Q., Liu, B., Wang, Y.-N., and Mao, H.: Air pollution in China: Status and spatiotemporal variations, Environ. Pollut., 227, 334–347, https://doi.org/10.1016/j.envpol.2017.04.075, 2017.

Song, Y., Wang, X., Maher, B. A., Li, F., Xu, C., Liu, X., Sun, X., and Zhang, Z.: The spatial-temporal characteristics and health impacts of ambient fine particulate matter in China, J. Clean. Product., 112, 1312–1318, https://doi.org/10.1016/j.jclepro.2015.05.006, 2016.

Tao, J., Gao, J., Zhang, L., Zhang, R., Che, H., Zhang, Z., Lin, Z., Jing, J., Cao, J., and Hsu, S.-C.: $PM_{2.5}$ pollution in a megacity of southwest China: source apportionment and implication, Atmos. Chem. Phys., 14, 8679–8699, https://doi.org/10.5194/acp-14-8679-2014, 2014.

U.S. EPA (Ed.): Guidance on the Use of Models and Other Analyses for Demonstrating Attainment of Air Quality Goals for Ozone, $PM_{2.5}$ and Regional Haze, Research Triangle Park, North Carolina, 2007.

Wang, L. T., Wei, Z., Yang, J., Zhang, Y., Zhang, F. F., Su, J., Meng, C. C., and Zhang, Q.: The 2013 severe haze over southern Hebei, China: model evaluation, source apportionment, and policy implications, Atmos. Chem. Phys., 14, 3151–3173, https://doi.org/10.5194/acp-14-3151-2014, 2014.

Wang, P., Ying, Q., Zhang, H., Hu, J., Lin, Y., and Mao, H.: Source apportionment of secondary organic aerosol in China using a regional source-oriented chemical transport model and two emission inventories, Environ. Pollut., 237, 756–766, https://doi.org/10.1016/j.envpol.2017.10.122, 2018.

Wang, P., Chen, K., Zhu, S., Wang, P., and Zhang, H.: Severe air pollution events not avoided by reduced anthropogenic activities during COVID-19 outbreak, Resour. Conserv. Recycl., 158, 104814, https://doi.org/10.1016/j.resconrec.2020.104814, 2020.

Wang, X., Li, L., Gong, K., Mao, J., Hu, J., Li, J., Liu, Z., Liao, H., Qiu, W., Yu, Y., Dong, H., Guo, S., Hu, M., Zeng, L., and Zhang, Y.: Modelling air quality during the EXPLORE-YRD campaign – Part I. Model performance evaluation and impacts of meteorological inputs and grid resolutions, Atmos. Environ., 246, 118131, https://doi.org/10.1016/j.atmosenv.2020.118131, 2021.

Wang, Y., Li, L., Chen, C., Huang, C., Huang, H., Feng, J., Wang, S., Wang, H., Zhang, G., Zhou, M., Cheng, P., Wu, M., Sheng, G., Fu, J., Hu, Y., Russell, A. G., and Wumaer, A.: Source apportionment of fine particulate matter during autumn haze episodes in Shanghai, China, J. Geophys. Res.-Atmos., 119, 1903–1914, https://doi.org/10.1002/2013JD019630, 2014.

Wang, Y., Zhu, S., Ma, J., Wang, P., Wang, P., and Zhang, H.: Enhanced atmospheric oxidation capacity and associated ozone increases during COVID-19 lockdown in the Yangtze River Delta, Sci. Total Environ., 768, 144796, https://doi.org/10.1016/j.scitotenv.2020.144796, 2021.

Yan, D., Lei, Y., Shi, Y., Zhu, Q., Li, L., and Zhang, Z.: Evolution of the spatiotemporal pattern of $PM_{2.5}$ concentrations in China – A case study from the Beijing-Tianjin-Hebei region, Atmos. Environ., 183, 225–233, https://doi.org/10.1016/j.atmosenv.2018.03.041, 2018.

Yang, W., Li, J., Wang, W., Li, J., Ge, M., Sun, Y., Chen, X., Ge, B., Tong, S., Wang, Q., and Wang, Z.: Investigating secondary organic aerosol formation pathways in China during 2014, Atmos. Environ., 213, 133–147, https://doi.org/10.1016/j.atmosenv.2019.05.057, 2019.

Yang, X., Xiao, H., Wu, Q., Wang, L., Guo, Q., Cheng, H., Wang, R., and Tang, Z.: Numerical study of air pollution over a typical basin topography: Source appointment of fine particulate matter during one severe haze in the megacity Xi'an, Sci. Total Environ., 708, 135213, https://doi.org/10.1016/j.scitotenv.2019.135213, 2020.

Yao, L., Yang, L., Yuan, Q., Yan, C., Dong, C., Meng, C., Sui, X., Yang, F., Lu, Y., and Wang, W.: Sources apportionment of $PM_{2.5}$ in a background site in the North China Plain, Sci. Total Environ., 541, 590–598, https://doi.org/10.1016/j.scitotenv.2015.09.123, 2016.

Ying, Q., Wu, L., and Zhang, H.: Local and inter-regional contributions to $PM_{2.5}$ nitrate and sulfate in China, Atmos. Environ., 94, 582–592, https://doi.org/10.1016/j.atmosenv.2014.05.078, 2014.

Yuan, Q., Qi, B., Hu, D., Wang, J., Zhang, J., Yang, H., Zhang, S., Liu, L., Xu, L., and Li, W.: Spatiotemporal variations and reduction of air pollutants during the COVID-19 pandemic in a megacity of Yangtze River

Delta in China, Sci. Total Environ., 751, 141820–141820, https://doi.org/10.1016/j.scitotenv.2020.141820, 2020.

Zhang, H., Li, J., Ying, Q., Yu, J. Z., Wu, D., Cheng, Y., He, K., and Jiang, J.: Source apportionment of $PM_{2.5}$ nitrate and sulfate in China using a source-oriented chemical transport model, Atmos. Environ., 62, 228–242, https://doi.org/10.1016/j.atmosenv.2012.08.014, 2012.

Zhang, H., Wang, Y., Hu, J., Ying, Q., and Hu, X. M.: Relationships between meteorological parameters and criteria air pollutants in three megacities in China, Environ. Res., 140, 242–254, https://doi.org/10.1016/j.envres.2015.04.004, 2015.

Zhang, H., Wang, S., Hao, J., Wang, X., Wang, S., Chai, F., and Li, M.: Air pollution and control action in Beijing, J. Clean. Product., 112, 1519–1527, https://doi.org/10.1016/j.jclepro.2015.04.092, 2016.

Zhang, R., Jing, J., Tao, J., Hsu, S.-C., Wang, G., Cao, J., Lee, C. S. L., Zhu, L., Chen, Z., Zhao, Y., and Shen, Z.: Chemical characterization and source apportionment of PM2.5 in Beijing: seasonal perspective, Atmos. Chem. Phys., 13, 7053–7074, https://doi.org/10.5194/acp-13-7053-2013, 2013.

Zhao, B., Wang, S., Donahue, N. M., Jathar, S. H., Huang, X., Wu, W., Hao, J., and Robinson, A. L.: Quantifying the effect of organic aerosol aging and intermediate-volatility emissions on regional-scale aerosol pollution in China, Sci. Rep., 6, 28815, https://doi.org/10.1038/srep28815, 2016.

Zheng, B., Tong, D., Li, M., Liu, F., Hong, C., Geng, G., Li, H., Li, X., Peng, L., Qi, J., Yan, L., Zhang, Y., Zhao, H., Zheng, Y., He, K., and Zhang, Q.: Trends in China's anthropogenic emissions since 2010 as the consequence of clean air actions, Atmos. Chem. Phys., 18, 14095–14111, https://doi.org/10.5194/acp-18-14095-2018, 2018.

Zheng, Y., Xue, T., Zhang, Q., Geng, G., Tong, D., Li, X., and He, K.: Air quality improvements and health benefits from China's clean air action since 2013, Environ. Res. Lett., 12, 114020, https://doi.org/10.1088/1748-9326/aa8a32, 2017.

Zhu, Y., Huang, L., Li, J., Ying, Q., Zhang, H., Liu, X., Liao, H., Li, N., Liu, Z., Mao, Y., Fang, H., and Hu, J.: Sources of particulate matter in China: Insights from source apportionment studies published in 1987–2017, Environ. Int., 115, 343–357, https://doi.org/10.1016/j.envint.2018.03.037, 2018.